Silver−Colloid−Nucleated Cytochrome c Superstructures Encapsulated in Silica Nanoarchitectures

ARTICLE *in* LANGMUIR · NOVEMBER 2004

Impact Factor: 4.46 · DOI: 10.1021/la048478u · Source: PubMed

6 AUTHORS, INCLUDING:

Kristin Eden
Virginia Polytechnic Institute and State Univ…
8 PUBLICATIONS **34** CITATIONS
SEE PROFILE

Rhonda M. Stroud
United States Naval Research Laboratory
343 PUBLICATIONS **6,410** CITATIONS
SEE PROFILE

Silver-Colloid-Nucleated Cytochrome *c* Superstructures Encapsulated in Silica Nanoarchitectures

Jean Marie Wallace, Brett M. Dening, Kristin B. Eden, Rhonda M. Stroud, Jeffrey W. Long, and Debra R. Rolison*

Surface Chemistry Branch (Code 6170) and Sensors and Materials Branch (Code 6360), Naval Research Laboratory, Washington, D.C. 20375

Received June 20, 2004. In Final Form: August 1, 2004

We recently discovered that self-organized superstructures of the heme protein cytochrome *c* (cyt. *c*) are nucleated in buffer by gold nanoparticles. The protein molecules within the superstructure survive both silica sol−gel encapsulation and drying from supercritical carbon dioxide to form air-filled biocomposite aerogels that exhibit gas-phase binding activity for nitric oxide. In this investigation, we report that viable proteins are present in biocomposite aerogels when the nucleating metal nanoparticle is silver rather than gold. Silver colloids were synthesized via reduction of an aqueous solution of Ag^+ using either citrate or borohydride reductants. As determined by transmission electron microscopy and UV−visible absorption spectroscopy, the silver nanoparticles vary in size and shape depending on the synthetic route, which affects the fraction of cyt. *c* that survives the processing necessary to form a biocomposite aerogel. Silver colloids synthesized via the citrate preparation are polydisperse, with sizes ranging from 1 to 100 nm, and lead to low cyt. *c* viability in the dried bioaerogels (∼15%). Protein superstructures nucleated at ∼10-nm Ag colloids prepared via the borohydride route, including citrate stabilization of the borohydride-reduced metal, retain significant protein viability within the bioaerogels (∼45%).

Introduction

Blending biofunction into the ultraporous nanoarchitectures known as aerogels has been limited by the inability of most biomolecules encapsulated in silica gels to survive the supercritical fluid processing necessary to convert the wet biomolecule−silica composite gel into the composite aerogel. The greatest success has been seen with lipase−silica composite aerogels,[1−3] but lipases are so rugged that they can catalyze enantioselective reactions at high temperatures in organic solvents.[4] The reason to invest the extra effort required to fabricate the sol−gel-derived composite architecture as an aerogel is that no compressive stresses arise during supercritical fluid processing, so the through-connected pore network innate to the wet gel is retained in the aerogel. The open porosity of the aerogel ensures that facile molecular transport persists in the air-filled three-dimensional nanoarchitecture.[5]

We recently succeeded in forming a biocomposite silica aerogel by "nanogluing" a self-organized cytochrome *c* (cyt. *c*) superstructure, depicted schematically in Figure 1, into the three-dimensional gel.[6] Nanoparticulate gold colloids nucleate the self-assembly of the protein superstructure in the liquid phase, which is then doped into an about-to-gel sol. The wet biocomposite gel is supercritically dried to form a mesoporous biocomposite aerogel[7] that presents advantages over previously reported bio-sol−gel-derived materials in that it need not be kept wet or stored at 4 °C to maintain protein viability.[8−10]

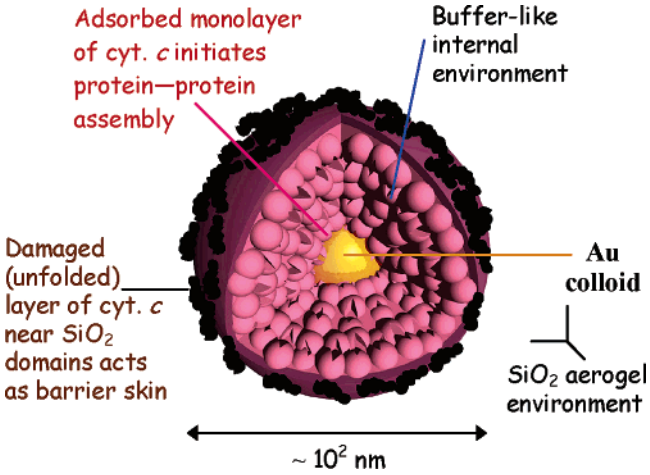

Figure 1. The model of a gold-nanoparticle-nucleated cytochrome *c* superstructure. The superstructure forms upon specific adsorption at the heme edge of the protein to the Au colloid followed by accretion of self-organized shells of additional protein molecules. A damaged boundary layer of protein is formed at the superstructure−silica interface as a result of the organic solvent-replacement steps and supercritical processing necessary to form an aerogel.

The heme protein survives the harsh conditions necessary to form an aerogel only in the presence of the nucleating nanoparticle.[7] Specific adsorption of a monolayer of cyt. *c* at colloidal gold in aqueous buffered media initiates formation of the stabilizing superstructure. This specifically oriented monolayer then rapidly assembles (in <10 s) the remaining protein in the buffered medium

* To whom correspondence may be addressed. E-mail: rolison@nrl.navy.mil. Tel: 202 767-3617. Fax: 202 767-3321.

(1) Antczak, T.; Mrowiec-Bialon, J.; Bielecki, S.; Jarzebski, A. B.; Malinowski, J. J.; Lachowski, A. I.; Galas, E. *Biotechnol. Tech.* **1997**, *11*, 9.
(2) Maury, S.; Buisson, P.; Pierre, A. C. *Langmuir* **2001**, *17*, 6443.
(3) El Rassy, H.; Maury, S.; Buisson, P.; Pierre, A. C. *J. Non-Cryst. Solids*, in press.
(4) Yasufuku, Y.; Shin-ichi Ueji, S.-I. *Bioorg. Chem.* **1997**, *25*, 88.
(5) Rolison, D. R. *Science* **2003**, *299*, 1698.
(6) Morris, C. A.; Anderson, M. L.; Stroud, R. M.; Merzbacher, C. I.; Rolison, D. R. *Science* **1999**, *284*, 622.
(7) Wallace, J. M.; Rice, J. K.; Pietron, J. J.; Stroud, R. M.; Long, J. W.; Rolison, D. R. *Nano Lett.* **2003**, *3*, 1463.
(8) Jin, W.; Brennan, J. D. *Anal. Chim. Acta* **2002**, *461*, 1.
(9) Dunn, B.; Miller, J. M.; Dave, B. C.; Valentine, J. S.; Zink, J. I. *Acta Mater.* **1998**, *46*, 737.
(10) Aylott, J. W.; Richardson, D. J.; Russell, D. A. *Chem. Mater.* **1997**, *9*, 2261.

10.1021/la048478u CCC: $27.50
Published on Web 09/18/2004

into a large superstructure, which is captured within the silica network upon gelation of the silica sol. The existence of this superstructure is verified by transmission electron micrographic analysis and postpyrolysis porosimetry.

While colloidal Au has been used extensively in bioconjugate chemistry, including with cytochrome *c*,[11,12] another prominent metal nanoparticle often used for biospectroscopy is silver. Silver demonstrates excellent SERS (surface-enhanced Raman scattering) enhancement and good biocompatibility, and it has been shown that cyt. *c* can bind to Ag colloids without denaturation.[13,14] The bioconjugates formed between Ag colloids and cyt. *c* indicate that the (sub)monolayer of protein binds to the Ag surface in a manner consistent with that on bulk, planar Au and Au colloids; i.e., the "front" heme edge of the protein, rich with cationic lysine residues, binds to the metal surface.[13] In analogy with our mechanism for colloidal Au-nucleated cyt. *c* superstructures, we posit that the specificity of cyt. *c* adsorption at high-curvature Ag nanoparticles should similarly initiate the self-organization of protein superstructures. As such protein superstructures are integral to the formation of biofunctional cyt. *c*−composite aerogels, viable composite bioaerogels should also be possible with Ag and not just Au colloids.

A critical difference between colloidal Au and colloidal Ag is that the latter is more difficult to prepare as monodisperse sols of a prespecified size. We describe herein the effect of different synthetic approaches to colloidal Ag and the effect of the resultant nanoparticles on the viability of cyt. *c* within aerogel-incorporated superstructures. Three synthetic variants were investigated for aqueous-phase reduction of silver nitrate to colloidal silver: sodium citrate; sodium borohydride; and sodium borohydride reduced, citrate stabilized. Protein superstructures derived from each type of nucleating silver nanoparticle are then doped into silica sol to form composite biogels, processed to form aerogels, and the viability of the heme protein is assessed by visible spectroscopy. The different preparations of the Ag colloids result in colloidal sols of varying properties that directly impact the amount of viable protein within the dry bioaerogel.

Experimental Section

Reagents. Cytochrome *c* (horse heart, type VI; Sigma Aldrich) was used as received. The concentrations of cytochrome solutions were calculated from their visible spectra using an extinction coefficient of 106 100 M^{-1} cm^{-1} for the Soret band.[15] Denaturation titrations were performed using a stock solution of 10 M guanidinium hydrochloride, GnHCl (Sigma-Aldrich). All reagents were used as received, unless otherwise noted; the water used in all experiments was 18 MΩ cm (Barnstead NANOpure).

Preparation of Silver Colloids. Our citrate synthesis is a modified Lee and Miesel preparation.[16] An aqueous solution of 0.036 g of $AgNO_3$ (Mallinckrodt) in 200 mL of water was sonicated for 10 min and then transferred to a microwave container. A 4-mL aliquot of aqueous 1% (w/v) sodium citrate (Alfa-AESAR) was added to the Ag^+ solution, and the mixture was microwave irradiated with a concomitant temperature ramp to 90 °C over a 5-min period (Mars 5 CEM Corp. Microwave). Heating was continued in 5-min intervals at a constant temperature of 90 °C, for a total irradiation time of 30 min. The pale yellow sol was then centrifuged (Hamilton Bell Van Guard V6500; 3400 rpm) for 30 min and the supernatant retained.

To synthesize borohydride-reduced colloids, an aqueous solution of sodium borohydride (15 mL, 1.2×10^{-3} M) was placed in a round-bottom flask in an ice bath. An aqueous solution of silver nitrate was prepared (1.8 mL, 2.2×10^{-3} M), iced, and then added to borohydride solution dropwise with continuous stirring.[17] The flask was removed from the ice and stirred in the dark for 45 min. The yellow sol was centrifuged for 45 min and the supernatant retained.

Citrate-stabilized, borohydride-reduced Ag colloids were prepared by adding a sodium citrate solution (1 mL, 4×10^{-3} M) dropwise to the borohydride-reduced sol (8 mL) after the initial 45 min of stirring.[17] The sol was then centrifuged for 45 min and the supernatant retained.

All Ag∼cyt. *c* experiments used freshly prepared Ag sol, with at most 30 min of storage in the dark at 4 °C. Sols to be analyzed by microscopy were also stored dark at 4 °C.

Preparation of Colloidal Silver∼Protein Superstructure. An aliquot of Ag sol was added to the stock cyt. *c* solution (∼0.7 mM, in a pH 7, 50 mM phosphate buffer) in a 5:1 volume ratio (i.e., 1.7 mL of colloidal Ag to 320 μL of cytochrome). The mixture was stirred for a minimum of 10 min; no separation techniques (i.e., centrifugation or filtration) were employed in order to prevent shear forces from disrupting the soft superstructure.

Preparation of the Silica Sol and Biocomposite Aerogel. The preparation of base-catalyzed silica sol was similar to that previously described.[6] First, 1.89 g of tetramethoxysilane (TMOS, Alfa AESAR, 98%) and 2.88 g of methanol (Mallinckrodt) were combined in a plastic beaker. Then, 0.75 g of water, 3 g of methanol, and 5 μL of 28% NH_4OH (99.99+%, Aldrich) were mixed in a second beaker. The TMOS solution was added to the second beaker, and the mixture was stirred for at least 15 min, after which the colloidal Ag∼cyt.*c* mixture was added to the silica sol in a 1:6 volume ratio and stirred for up to 2 min. The Ag∼cyt.*c*−silica mixture was poured into cylindrical polypropylene molds (13-mm diameter, × 57 mm) and sealed with Parafilm. The gels were aged for 1 day at 4 °C, transferred to glass vials, and rinsed with ethanol (Warner-Graham Co.) at least four times over 1.5 days. The gels were rinsed with acetone (Fisher Scientific) at least eight times over 3 to 4 days and loaded into a supercritical dryer (Polaron Range; Quorum Technologies Newhaven, East Sussex), where the acetone was replaced with liquid CO_2. The liquid CO_2 was brought above its critical temperature and pressure (T_c = 31 °C; P_c = 7.4 MPa) and vented. The aerogels are translucent peach in appearance, and shrinkage during the drying process is minimal.

Physical Characterization. The UV−visible spectra for the Ag colloidal sol, Ag∼cyt. *c* buffered media, and Ag∼cyt.*c*−SiO_2 aerogels were obtained using a photodiode single-array spectrophotometer (Agilent model 8453). The microscopic analyses were performed on a JEOL 2010F field-emission transmission electron microscope equipped with a Gatan 794 MSC CCD camera. To avoid sample preparation artifacts associated with solvents and grinding, sub-millimeter flakes, extracted from the interior of the aerogel monolith using a razor blade, were attached directly to Cu-mesh transmission electron microscopy (TEM) grids. Electron-beam damage during TEM analysis was minimized by using low beam currents and by observing the sample with a CCD camera. Aliquots of silver colloidal sol were syringed onto holey carbon film for TEM analysis.

Fluorescence measurements were obtained with a Fluorolog Spex (1681 0.22 m spectrometer and 1680 0.22 m double spectrometer). Emission scans of 310−450 nm were recorded after excitation at 295 nm. Solutions (cyt. *c*, Ag sol, water, buffer, and GnHCl), were filtered with Teflon 0.45-μm syringe filters (Fisherbrand). After filtering, the biocomposite was mixed as described above. Initial emission scans were recorded for the Ag∼cyt. *c* composite and for a cyt. *c* control, and then the solutions were spiked with 10 M GnHCl, and additional emission scans were recorded for the unfolded protein.

Results and Discussion

Synthetic Variants to Silver Nanoparticle Colloids. The preparation of silver colloids is sensitive to

(11) Keating, C. D.; Kovaleski, K. M.; Natan, M. J. *J. Phys. Chem. B* **1998**, *102*, 9404.
(12) Keating, C. D.; Kovaleski, K. M.; Natan, M. J. *J. Phys. Chem. B* **1998**, *102*, 9414.
(13) Hildebrandt, P.; Stockburger, M. *J. Phys. Chem.* **1986**, *90*, 6017.
(14) Macdonald, I. D. G.; Smith, W. E. *Langmuir* **1996**, *12*, 706.
(15) Margoliash, E.; Frohwirt, N. *Biochem. J.* **1959**, *71*, 570.
(16) Lee, P. C.; Meisel, D. *J. Phys. Chem.* **1982**, *86*, 3391.
(17) Keir, R.; Sadler, D.; Smith, W. E. *Appl. Spectrosc.* **2002**, *56*, 551.

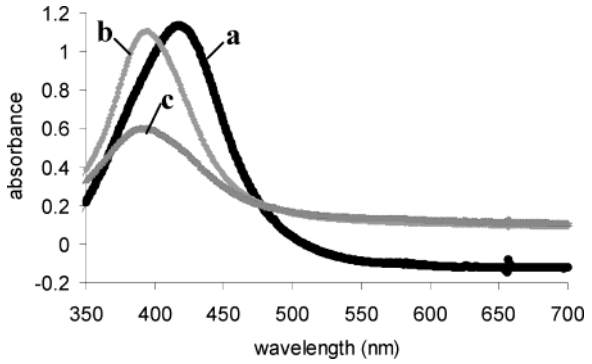

Figure 2. Ultraviolet−visible spectra of the silver colloids produced from (a) citrate reduction, (b) sodium borohydride reduction, and (c) citrate-capped borohydride reduction.

many experimental factors including temperature, extent of mixing, and rate of addition of reactants.[17,18] As a result, it is difficult to prepare stable colloids in a reproducible manner using a batch process. The formation of Ag nanoparticles can be tracked by both color change and UV−visible spectra of the solutions, with the peak position, shape, and full-width at half-maximum (fwhm) of the plasmon band strongly dependent on the size and shape of the nanoparticles. The position of the plasmon band indicates the average particle size of the metal nanoparticle while the fwhm correlates with the particle size distribution (polydispersity yields large fwhm's).

We initially chose the citrate-reduction synthetic route,[16] but used microwave irradiation to shorten the time of preparation and to control the heating in the expectation that the resultant colloids would be more monodisperse in size and shape. It has been shown that time of heating controls the size of Ag colloids as prepared by either traditional[18] or microwave heating.[19,20] In an earlier study, large (60−80 nm) Ag particles formed after only 2 min of heating, characterized by a spectrum with a plasmon maximum at 413 nm and a fwhm of 89 nm. After 45−90 min of heating, a monodisperse sol of smaller (10−20 nm) particles formed (λ_{max} 402−404 nm, fwhm 53−57 nm) that was stable for 2 months.[18]

Figure 2a shows the transmission visible spectrum of the resultant sol using the citrate/microwave protocol. Although the plasmon peak position for citrate-prepared Ag colloids can vary greatly from lab to lab (406−450 nm), we observed a plasmon maximum at 418 nm, very similar to the reported plasmon maximum of 420 nm for the procedure we modified.[16] Our citrate-reduced product did not, however, comprise colloidal particles with a narrow size distribution as the fwhm is ∼86 nm (Figure 2a). Both the average peak position and fwhm of the surface plasmon band indicate that the Ag particles within the sol are polydisperse in size and shape.[18]

The TEM analysis of freshly prepared, citrate-derived Ag sol (Figure 3a) supports the findings of the spectroscopy. As seen in the micrograph, the size of the nanoparticles ranges from 1 to 100 nm and the nanoparticles form in a multitude of shapes. Therefore, our attempts to control the size and shape distribution through microwave irradiation were not successful.

Several reports describe using stabilizers during formation of a Ag sol as a means to control particle aggregation and morphology. A common stabilizer, PVP (poly(*N*-vinyl-2-pyrrolidine)) has been used to produce both

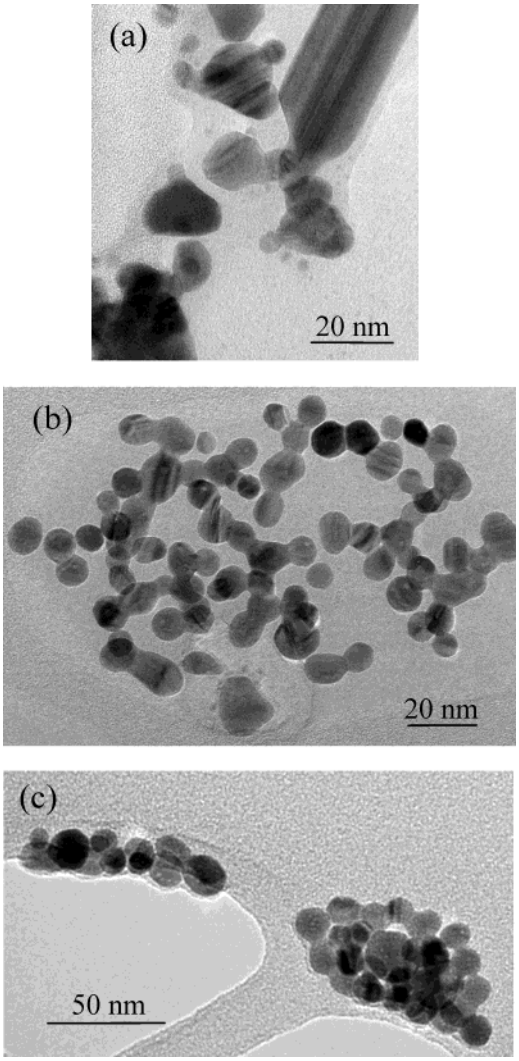

Figure 3. Transmission electron micrographs of silver colloids produced from (a) citrate reduction, (b) sodium borohydride reduction, and (c) citrate-capped borohydride reduction.

well-defined Ag nanoparticles[19] and Ag dendrites[20] under microwave irradiation. However, we did not want to greatly modify the surface of the Ag nanoparticle and possibly interfere with cyt. *c* adsorption.

A more reproducible means to synthesize electrostatically stabilized Ag colloids, with better control of the morphology, has been via sodium borohydride reduction (denoted simply as $NaBH_4$).[17] Colloidal nanoparticles formed by this route tend to have smaller size distributions, with typical spectra for 10-nm particles displaying a peak maximum at 391 nm and a fwhm of 52 nm.[17] These values are similar to what we observe for our borohydride-prepared Ag sols; the average plasmon maximum for these colloids (395 nm) blue shifts compared to the citrate colloids and exhibits a narrowed fwhm (∼68 nm) (see Figure 2b).

We also wanted to combine the batch-to-batch reproducibility and narrow size distribution of the $NaBH_4$ procedure with the stability of the citrate procedure. We "capped" the surface of the $NaBH_4$ colloids through addition of citrate salts after the initial colloid formation, and the resultant spectrum is shown in Figure 2c (average plasmon maximum, λ_{max}, at 392 nm, and fwhm ∼85 nm). The TEM analysis indicates that both the $NaBH_4$ and $NaBH_4$-reduced, citrate-capped colloidal sols contain smaller particles, 10 ± 1.6 and 13 ± 3.3 nm, respectively, than the citrate preparation (Figure 3). These borohydride-reduced nanoparticles are also more uniform in shape

(18) Munro, C. H.; Smith, W. E.; Garner, M.; Clarkson, J.; White, P. C. *Langmuir* **1995**, *11*, 3712.
(19) He, R.; Qian X.; Yin, J.; Zhu, Z. *J. Mater. Chem.* **2002**, *12*, 3783.
(20) He, R.; Qian X.; Yin, J.; Zhu, Z. *Chem. Phys. Lett.* **2003**, *369*, 454.

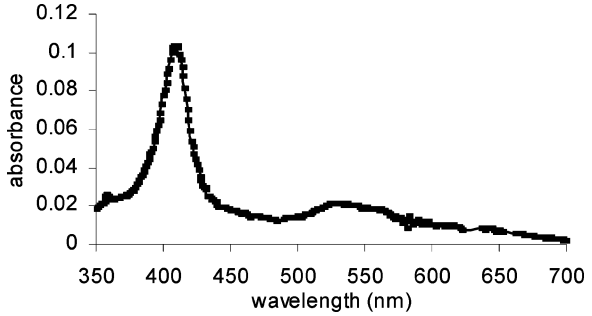

Figure 4. Ultraviolet−visible spectrum of the Ag∼cyt. *c* protein superstructure in buffered media. The absorption at 500−575 nm arises from the sidebands of the cytochrome.

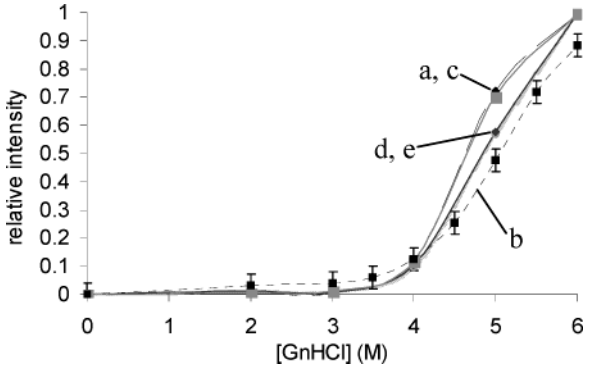

Figure 5. Fluorescence spectra for titration of the following media with guanidinium hydrochloride: (a) cyt. *c*; (b) 10-nm Au∼cyt. *c* (data derived from ref 7); (c) citrate Ag∼cyt. *c*; (d) $NaBH_4$ Ag∼cyt. *c*; and (e) citrate-capped $NaBH_4$ Ag∼cyt. *c*.

than the citrate-prepared colloids, although some sintering is evident for the noncapped $NaBH_4$ sample.

Keir et al. observed a plasmon maximum at 396 nm, 60-nm fwhm, and size distributions of 7−60 nm for $NaBH_4$−reduced/citrate-capped Ag colloids.[17] These authors attribute the range of particle sizes to different mixing regimes in their flow system. We did the capping by batch process and observed a more narrow size distribution by TEM (13 ± 3.3 nm), although similar spectral characteristics were obtained. This sol should have a number density of $\sim 2 \times 10^{13}$ particles per mL (as calculated from the TEM-derived particle size and total number of Ag atoms).

Silver∼cyt. *c* Biocomposite. Formation of the Ag∼cyt. *c* composite followed the method we developed for the Au∼cyt. *c* composite. Fresh Ag colloidal sol was mixed with a stock solution of cyt. *c* in a 5:1 Ag sol/cyt. *c* volume ratio. Figure 4 shows a representative visible spectrum of the buffered composite medium.

While cyt. *c* adsorbs to Ag colloids without denaturation,[13,14] one concern was that the position of the Ag plasmon band in the transmission spectra would mask the Soret band of the cyt. *c*, which we use to establish the viability of the heme protein. As can be seen in Figure 4, the Soret band at 409 nm dominates the spectrum, with no distinguishable Ag plasmon band. Previous work with Ag colloids noted the marked attenuation of the Ag surface plasmon (>50% loss of signal intensity) upon adsorption of even a monolayer of cyt. *c*.[12,21] With adsorption of multilayers of protein, the loss of the surface plasmon of the Ag colloid is realistic.

The Soret peak for cyt. *c* in the presence of Ag nanoparticles does not shift in wavelength relative to the native protein in buffered solution. In addition, there is no loss of signal intensity for cyt. *c* in the composite indicating that no denaturation of the protein occurs upon exposure to the Ag colloidal sol. Similar spectra, i.e., dominated by the cyt. *c* absorptions, were obtained for biocomposites formed from all three types of Ag colloids synthesized for this study.

Chemically induced unfolding experiments were performed by serial titrations of the Ag∼cyt. *c* composite medium with 10 M GnHCl. The fluorescence emission from the tryptophan-59 of cyt. *c* critically depends on the conformational integrity around the heme,[22] whereby the heme completely quenches the Tyr-59 fluorescence when cyt. *c* is in its native configuration. Figure 5 shows the change in protein fluorescence as a function of GnHCl concentration for cyt. *c* in buffer, 10-nm Au∼cyt. *c* composite, and Ag∼cyt.*c* composites. As we have previously shown, a stabilization of the protein occurs in the presence of 10-nm Au colloids, as indicated by the midpoint of unfolding shifting by 0.2 M units toward higher concentrations of GnHCl.[7] With the freshly prepared citrate Ag sol, no such stabilization occurs as the fluorescence (and therefore the degree of unfolding) closely tracks that of the buffered cyt. *c*.

This lack of an effect is most likely due to the large size range of particles within the colloidal sol. We have observed similar diminished stabilization as the size of the nanoparticle within the Au∼protein superstructure is increased, with larger Au colloids, i.e., >70 nm, showing no stabilization in the presence of GnHCl.[23]

In contrast, the response for the composite composed of Ag nanoparticles formed from the more monodisperse $NaBH_4$ or $NaBH_4$-reduced/citrate-capped colloidal sols resembles the response for the 10-nm Au composite in that a shift in the protein unfolding to higher concentrations of GnHCl occurs in the presence of the metal colloid. However, this shift, while representing a stabilization of protein within these Ag-nucleated superstructures, does not occur to the same extent as for the 10-nm Au-directed superstructures. This difference may be due to the varied morphology of the Ag nanoparticles. The commercial Au sol used previously contained spherical Au nanoparticles with a known volume density of particles.[7,23,24] Here, our Ag colloids vary in shape and we would expect this variation to alter the formation and stability of the protein−protein interactions of the superstructure.

Silver∼cyt. *c* Biocomposite Aerogels. Greater than 80% of the initial Soret intensity of cyt. *c* in solution is preserved for encapsulated cyt. *c* in supercritically dried silica aerogel when the protein is preassociated with 10-nm colloidal Au.[7] If the protein is not preassociated with colloidal gold, none of the cyt. *c* survives the processing necessary to form an aerogel, as indicated by the disappearance of the visible Soret band. The viability of the protein contained within a nanoglued, preassociated Ag∼cyt. *c*−silica aerogel can be similarly measured.

The metal−protein composite was captured from the buffered medium by adding an about-to-gel silica sol to form a composite gel. The response of the proteins to the various processing conditions while encapsulated within the silica nanoarchitecture was monitored using the Soret peak in the transmission spectra and is shown in Figure 6. All spectra exhibit only a minor shift in Soret position

(21) Sibbald, M. S.; Chumanov, G.; Cotton, T. M. *J. Phys. Chem.* **1996**, *100*, 4672.
(22) Tsong, T. Y. *Biochemistry* **1976**, *15*, 5467.
(23) Wallace, J. M.; Rolison, D. R. Unpublished results, Naval Research Laboratory, 2003.
(24) Wallace, J. M.; Stroud, R. M.; Pietron, J. J.; Long, J. W.; Rolison, D. R. *J. Non-Cryst. Solids*, in press.

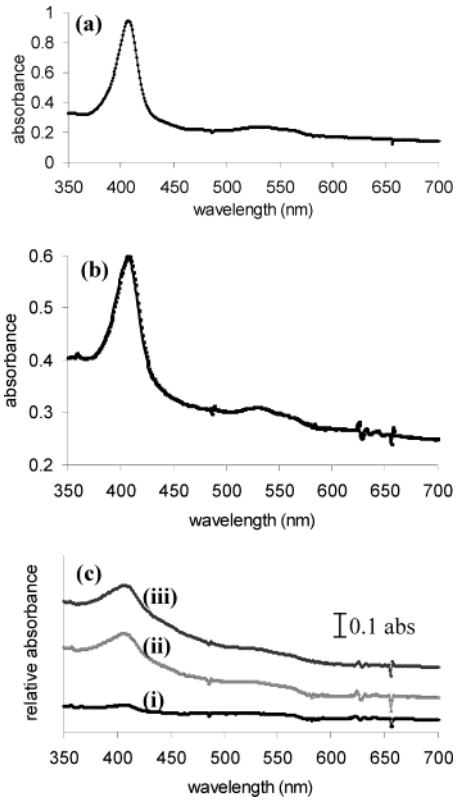

Figure 6. Ultraviolet−visible spectra for Ag∼cyt. *c*−silica incorporated into (a) wet gel in the sol−gel mother liquor (citrate-prepared Ag colloid); (b) wet gel in buffered medium (citrate-prepared Ag colloid); and (c) aerogel at room temperature where the Ag colloid was prepared via (i) citrate reduction; (ii) $NaBH_4$ reduction; and (iii) $NaBH_4$ reduction with citrate capping, spectra offset for clarity.

(405−407 nm) compared to cyt. *c* in solution (409 nm), but the amount of viable cyt. *c* is less at each processing stage, as indicated by a decrease in the volume-normalized absorbance.

During gelation of the composite gel, we observe a 17% decrease in viability upon exposure of the Ag∼cyt. *c* components to the alcohol-rich silica sol−gel recipe, while for the biocomposite gel soaked in buffer (before rinsing with acetone) 63% of the protein remains viable. We would expect that these decreases are in response to the harsh chemical and physical conditions necessary to form the gels. As noted in the fluorescence studies, the presence of colloidal Ag is not as stabilizing to the cytochromes in the superstructure as is the presence of Au nanoparticles.

Likewise upon exposure of the composite biogel to organic solvents during rinsing, an additional decrease in protein viability is noted; yet another loss occurs upon supercritically drying the wet gel to form the aerogel. For dry biocomposite aerogels, the viability of the cyt. *c* depends on the type of Ag colloid incorporated within the superstructure**.** The Soret intensity obtained for bioaerogels formed from superstructures nucleated with either the $NaBH_4$ or $NaBH_4$-reduced/citrate-capped Ag colloids indicates that 45% of the cyt. *c* retains viability.

In contrast, for a biocomposite aerogel formed from the citrate-prepared Ag sols, only 15% of the protein retains viability (as determined from the spectra).[25] This decrease in cyt. *c* stability is most likely due to the large range of sizes and shapes of the Ag colloids used to nucleate the protein−protein self-assembly. Analogously to our fluorescence results, increasing the size of Au nanoparticles above a threshold limit (>70 nm) alters the packing around the nanoparticle and appears to destabilize the protein−protein interactions so crucial to superstructure formation.[23] This destabilization of the protein superstructure correlates with the degree of loss of protein viability upon supercritical-fluid processing to form the dried nanoarchitecture. No aggregation is observed upon mixing the borohydride-reduced metal nanoparticles sol with the protein, but significant precipitation is observed when silica sol is added to Ag∼cyt. *c* composites derived from citrate-synthesized Ag colloids. This deleterious interaction is most likely due to protein-induced aggregation of the Ag nanoparticles.

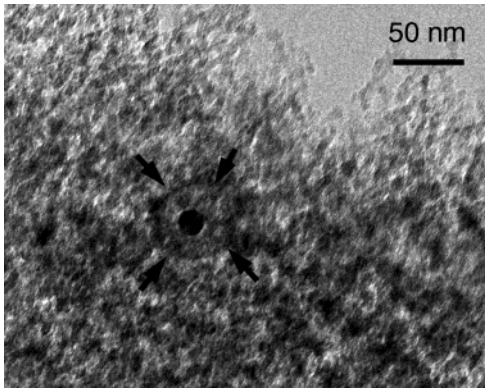

Figure 7. Transmission electron micrograph of Ag∼cyt. *c*−SiO_2 composite aerogel. The Ag colloid is seen as the solid black object surrounded by the radially symmetric protein shells. Arrows have been added at points along the edge of the superstructure to guide the eye.

Figure 7 shows a typical transmission electron micrograph of a citrate-capped $NaBH_4$ Ag∼cyt. *c*−SiO_2 bioaerogel. We observe no evidence of Ag agglomeration in this sample or of damaged protein. The dark circle (∼16 nm) is the Ag nanoparticle. The protein surrounding the Ag nanoparticle in the superstructure (with a diameter of 57 nm) is slightly darker than the silica of the aerogel host. This image (and related structures observed in this sample) supports our spectroscopic data, which indicate that less of the initial cyt. *c* remains viable in the Ag-nucleated biocomposite aerogel (as compared with Au-nucleated superstructures). The Ag-nucleated superstructures are smaller than those obtained by nucleating cyt. *c* superstructures with 10-nm Au (∼7 vs 11 shells of cyt. *c*) and consequently they have a higher surface-to-volume ratio than the previously reported Au-nucleated superstructures.[7] In our superstructure model, the outermost layer(s) of protein serves as a damaged, "sacrificial skin". The higher the surface-to-volume ratio of the protein superstructure, the more denatured protein there will be associated with each superstructure.

On the basis of our work with cyt. *c* and variously sized Au colloids, we observed with Ag what we had predicted: more cyt. *c* survives the sol−gel and supercritical processing when using $NaBH_4$-derived, rather than citrate-derived Ag colloids to nucleate protein superstructures because the $NaBH_4$-derived colloidal sols consist of small nanoparticles with a narrow size distribution.

(25) Ag∼cyt. *c* superstructures and biocomposite aerogels were also nucleated with commercial citrate Ag colloids (20 nm, Ted Pella). No improved stability was noted by the fluorescence studies in buffered medium; the response tracked that for mixing our in-house prepared citrate Ag colloids with cyt. *c* in buffer. While on average, 32% of the encapsulated protein remained viable with the commercial sol, the range of actual viable protein within the biocomposite aerogel was 11−62%. We observe little stabilization using the commercially available Ag colloidal sol, and the results are not reproducible batch-to-batch.

Conclusion

We have shown that Ag nanoparticles direct the self-assembly of protein superstructures, and the resulting superstructures can be encapsulated in silica aerogels while retaining the viability of the protein. This study successfully extends our strategies for stabilizing proteins as previously reported with Au nanoparticles as the nucleating agent. The stability of cyt. *c* in both buffered media and the Ag∼cyt. *c*−silica biocomposite aerogels is strongly affected by the size and shape dispersity of the Ag nanoparticles. Biocomposite aerogels with high cyt. *c* viability are only achieved when the Ag nanoparticles are introduced with small sizes (∼10 nm) and limited size dispersity.

Acknowledgment. We gratefully acknowledge the support of this work by the U.S. Office of Naval Research and extend our thanks to our NRL colleagues, Greg Collins, for use of the fluorimeter, and Michael Doescher, for preparing the model of the Au-nucleated protein superstructure. J.M.W. is an NRC-NRL Postdoctoral Associate (2000−2004).

LA048478U